Protist, Vol. 164, 793–810, November 2013
http://www.elsevier.de/protis
Published online date 23 October 2013

Protist

ORIGINAL PAPER

Fusiforma themisticola n. gen., n. sp., a New Genus and Species of Apostome Ciliate Infecting the Hyperiid Amphipod *Themisto libellula* in the Canadian Beaufort Sea (Arctic Ocean), and Establishment of the Pseudocolliniidae (Ciliophora, Apostomatia)

Chitchai Chantangsi[a,1], **Denis H. Lynn**[b,c], **Sonja Rueckert**[d], **Anna J. Prokopowicz**[e], **Somsak Panha**[a], and **Brian S. Leander**[f]

[a]Department of Biology, Faculty of Science, Chulalongkorn University, Phayathai Road, Pathumwan, Bangkok 10330, Thailand
[b]Department of Zoology, University of British Columbia, Vancouver, BC V6T 1Z4, Canada
[c]Department of Integrative Biology, University of Guelph, Guelph, ON N1G 2W1, Canada
[d]School of Life, Sport and Social Sciences, Edinburgh Napier University, Sighthill Campus, Sighthill Court, Edinburgh EH11 4BN, Scotland, United Kingdom
[e]Québec-Océan, Département de Biologie, Université Laval, Quebec, QC G1V 0A6, Canada
[f]Canadian Institute for Advanced Research, Departments of Zoology and Botany, University of British Columbia, Vancouver, BC V6T 1Z4, Canada

Submitted May 30, 2013; Accepted September 16, 2013
Monitoring Editor: Genoveva F. Esteban

A novel parasitic ciliate *Fusiforma themisticola* n. gen., n. sp. was discovered infecting 4.4% of the hyperiid amphipod *Themisto libellula*. Ciliates were isolated from a formaldehyde-fixed whole amphipod and the DNA was extracted for amplification of the small subunit (SSU) rRNA gene. Sequence and phylogenetic analyses showed unambiguously that this ciliate is an apostome and about 2% divergent from the krill-infesting apostome species assigned to the genus *Pseudocollinia*. Protargol silver impregnation showed a highly unusual infraciliature for an apostome. There are typically 8 (6-9) bipolar somatic kineties covering the banana-shaped body. The anterior end of the oral cavity begins about 1/3 of the body length from the anterior end and is composed of an inpocketing that is lined on its anterior and left wall with an oral field of densely packed ciliated kinetosomes. Stomatogenesis begins with some dedifferentiation of the parental oral field and elongation of its paroral and oral kineties. A new

[1]Corresponding author; fax +66-2-218-5386
e-mail Chitchai.C@chula.ac.th (C. Chantangsi).

http://dx.doi.org/10.1016/j.protis.2013.09.001

oral field develops midventrally and the paroral and oral kineties break to form the oral apparatus of the opisthe, which completes development by additional kinetosomal proliferation and migration of the paroral. This morphology is novel among apostomes and justifies the establishment of a new genus and species.

Key words: Alveolata; Crustacea; exuviotrophy; Hyperiidae; parasite; SSU rDNA.

Introduction

The Ciliophora is a monophyletic assemblage of protists occupying a wide range of ecological habitats and exhibiting a diverse array of biological lifestyles, ranging from free-living to parasitic species (Lynn 2008). A parasitic lifestyle occurs in several different lineages of ciliates [e.g., apostomatids, chilodonellids, holophryids, ichthyophthiriids, trichodinids, etc.] and is reported regularly to cause mild to lethal disease in both invertebrates and vertebrates (Arthur and Lom 1984; Dickerson and Dawe 1995; Fernandez-Leborans and Tato-Porto 2000; Hoffman 1988; Landers 2010; Lom 1995). Although parasitism is sometimes useful in controlling populations of some undesired organisms, like pests, it can be a major cause of losses if such parasites infect economically important organisms, such as shrimps, lobsters, crabs, and fishes (Pérez 2009). In addition, parasites can sometimes interfere with the stability of food chains and food webs, if they reach high intensities and prevalences (Pérez 2009). For example, parasitoid ciliates of marine planktonic crustaceans, particularly apostome ciliates, can have dramatic impacts on host mortality and in doing so influence trophic links in planktonic food webs (Gómez-Gutiérrez et al. 2003, 2012).

In a survey of the parasites of the pelagic hyperiid amphipod *Themisto libellula* in the Canadian Beaufort Sea, Prokopowicz et al. (2010) reported on two parasites that were commonly encountered in this significant trophic link: (1) 60.2% of the hosts were infected by the gregarine *Ganymedes themistos*, and (2) 4.4% of the hosts had an unidentified ciliate in the haemolymph. These authors found that for a given size of host there were higher infections of ciliates in sediment traps (16.3% vs. 6%), suggesting that the ciliates may have killed the hosts.

In this report, we characterized the morphology and stomatogenesis of this parasitic ciliate, which we named *Fusiforma themisticola* n. gen., n. sp., and analyzed its molecular phylogenetic position using small subunit (SSU) rRNA gene sequences. Both morphological and molecular phylogenetic data demonstrated the relationship between this species and the recently described apostome species, assigned to the new genus *Pseudocollinia*, which are parasitoids that kill krill in the Eastern Pacific Ocean (Gómez-Gutiérrez et al. 2012). Because the morphological traits shared by *Pseudocollinia* and *Fusiforma* n. gen. are so distinct from other colliniid ciliates that infect the haemolymph of crustaceans, we also established the new family Pseudocolliniidae n. fam. to include these apostomes.

Results

General Morphology

Fusiforma themisticola n. gen., n. sp. (Figs 1-6, Table 1)

Description: This ciliate is spindle-shaped and thin, typically with pointed anterior and posterior ends and with a slight bend, appearing somewhat banana-shaped (Figs 1, 3, 4). Non-dividers were variable in length, ranging from 28-121 μm (N = 116) (Table 1), but more consistent in body width, ranging from 9-24 μm (N = 116) (Table 1). Only one morphotype was observed and it typically had 8 (N = 115) (Table 1) bipolar somatic kineties, which were often slightly more closely spaced on the ventral surface (Figs 1, 3, 4). The kinetosomes of the somatic kineties were densely packed and apparently all were ciliated (Figs 2, 4). Scattered along the kineties were what appeared to be swollen vesicles, perhaps parasomal sacs (arrows, Fig. 4A). The macronucleus typically extended from the anterior to the posterior end of the cell, ranging in length from 21-116 μm (N = 115) and in width from 4-17 μm (N = 116) (Table 1). It often appeared to be swollen as it had several bends in it (Figs 1, 3, 4). It is not known whether this was an artifact of the formaldehyde-fixation. A micronucleus could not be identified.

The anterior end of the oral cavity, which defines the beginning of the oral region, was 7-46 μm (N = 86) or about 1/3 of the body length from the anterior end (Figs 1-4; Table 1). The oral cavity was invaginated as a cone- or cup-shaped depression on whose left anterior and dorsal walls was a dense

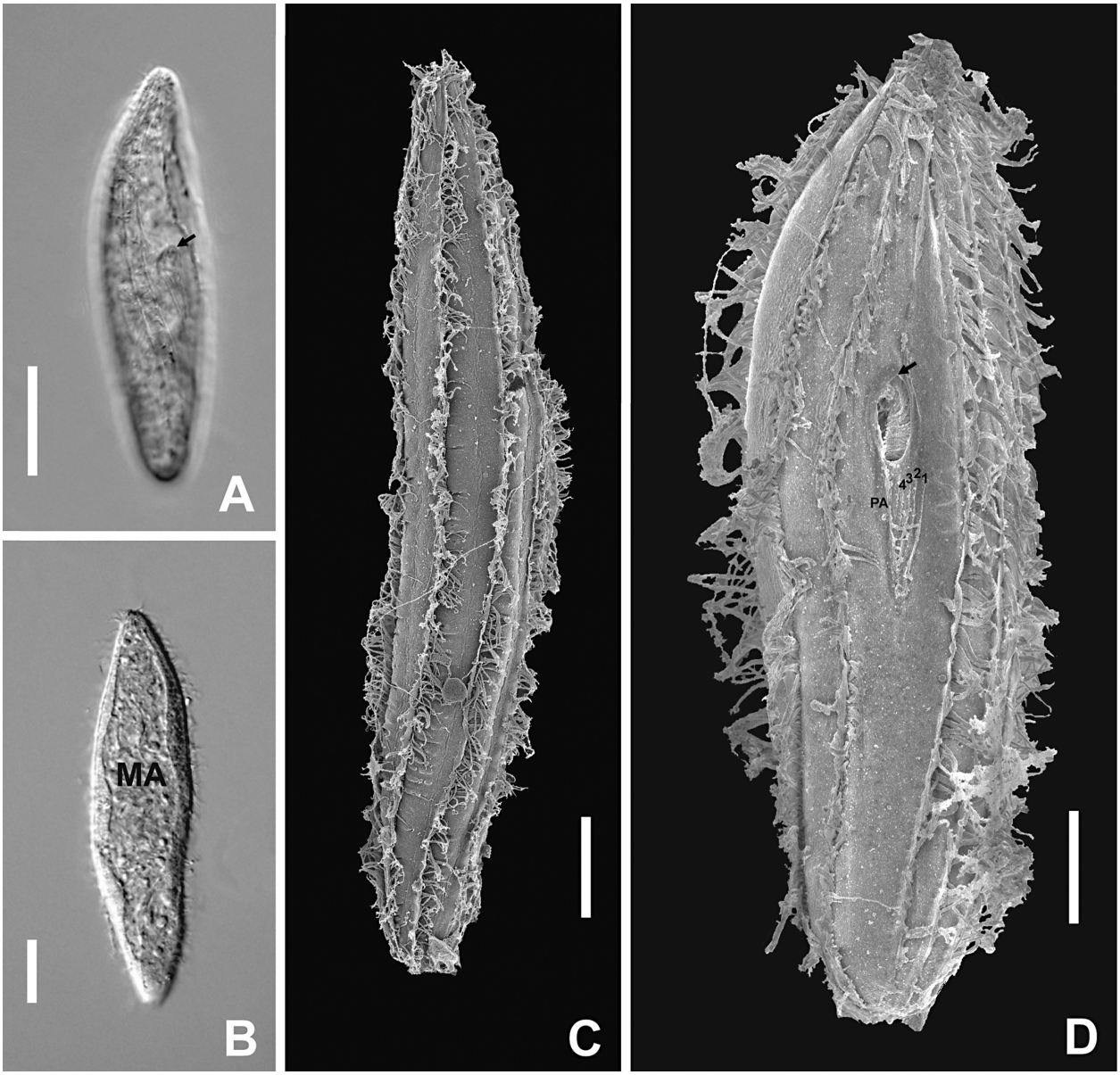

Figure 1. Light and scanning electron micrographs of *Fusiforma themisticola* n. gen., n. sp. **A**-**B**. Light micrographs of the cell surface showing kineties (A) and a focal plane showing the swollen macronucleus (MA) (B). The anterior border of the oral cavity is indicated by the arrow. **C**-**D**. Scanning electron micrographs of the dorsal surface showing the densely ciliated and widely spaced kineties (C) and of the ventral surface showing the oral region (arrow) located about 1/3 distance from the pointed anterior end (D). There are ridges on the cell surface, posterior to the oral cavity, which after protargol staining are interpreted as a paroral (PA) and in this specimen 4 left oral kineties. [Scale bars, A = 40 μm; B = 15 μm; C = 16 μm; D = 10 μm].

field of ciliated kinetosomes (Figs 1-4). Four other oral kineties were observed and these were apparently not ciliated (Figs 1, 2). On the right side of the oral region, apparently encircling the anterior edge of the oral cavity and then extending posteriorly on the right was a paroral (Figs 3, 4). On the left side of the oral region, there were typically 3±0.66 (N = 116) oral kineties that extended somewhat obliquely to the right from the posterior left side of the oral opening (Figs 1-4). We have numbered these 1, 2, and 3, from left to right, but they could range up to 5 in number (Figs 3, 4; Table 1).

Stomatogenesis: About half the cells encountered were undergoing cell division. Dividers

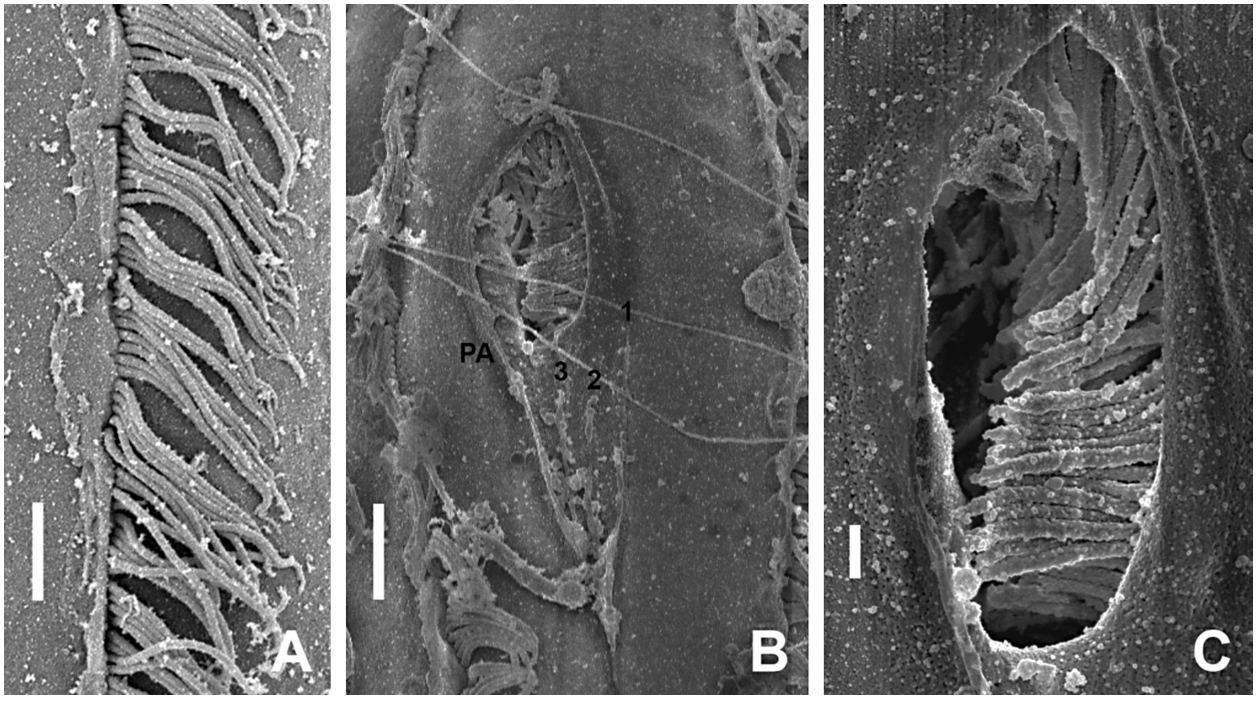

Figure 2. Scanning electron micrographs of *Fusiforma themisticola* n. gen., n. sp. **A**. Detail of a somatic kinety showing dense packing of cilia. **B**. Oral region with an anterior concavity behind which is a triangular-shaped region that has perhaps 4 ridges, corresponding to the paroral (PA) on the right and three left oral kineties, numbered 1, 2, and 3. **C**. Detail of the oral cavity illustrating the densely ciliated left and anterior walls. Since the somatic cilia (A) and oral cavity cilia (C) are preserved, it is assumed that the absence of cilia from the paroral and left oral kineties is not an artifact of fixation. [Scale bars, A = 2.5 μm; B = 3 μm; C = 0.6 μm].

ranged in length from 26-85 μm (N = 125) (Table 1). Early dividers were identified by proliferation of kinetosomes in the posterior half of the paroral, forming an anarchic field of kinetosomes (Figs 3F, 5A, 6A). Some very small dividers were observed whose oral regions had reduced numbers of kinetosomes (Fig. 4C). This suggests that once division began, there may have followed one or two subsequent divisions without intervening cell growth and perhaps reduced kinetosomal replication. The oral field appears to elongate as kinetosomes of the oral kineties separate and replicate, ultimately separating the proter and opisthe oral anlage (Figs 5, 6). At the fullest extent of separation, the oral apparatus of the proter has dedifferentiated to a state similar to that of the

Table 1. Morphometric characterization of the apostome ciliate *Fusiforma themisticola* n. gen., n. sp., infecting the hyperiid amphipod *Themisto libellula* in the Canadian Beaufort Sea (Arctic Ocean).

Character	Mean	S.D.	Range	N
Non-Dividers				
Body length, μm	72.6	17.2	28-121	116
Body width, μm	16.7	2.5	9-24	116
Number of somatic kineties	8	0.56	6-9	115
Macronuclear length, μm	66.5	17.0	21-116	115
Macronuclear width, μm	10.2	2.9	4-17	116
Distance from anterior pole to anterior of oral cavity, μm	24.7	7.6	7-46	86
Number of left oral kineties	3	0.66	2-5	116
Dividers				
Body length, μm	80.3	17.6	26-85	125

Figure 3. Protargol stains of non-dividing *Fusiforma themisticola* n. gen., n. sp. **A**-**B**. Two cells showing range of placement of the oral region from anterior one-third (A) to almost equatorial (B). The paroral (PA) and 3 or 4 left oral kineties are visible in these specimens. **C**. Oral region in focus showing a paroral (PA) on the right of the oral cavity and three obliquely oriented oral kineties (1, 2, 3) to the left and posterior of the oral cavity. **D**. Focal plane through two cells of very different size showing the large macronucleus (MA) extending from pole to pole. The size difference suggests that once division begins, it is a palintomic process (see also Fig. 4C). **E**. Focal plane showing the cup- or cone-shaped oral cavity (OC). **F**. Focal plane through the oral cavity of an early divider, showing the dense oral ciliature on the left and anterior of the oral cavity walls, the anarchic field (AF) of kinetosomes (see also Fig. 6A), and four left oral kineties (1, 2, 3, 4) whose kinetosomes are separating as an early sign of stomatogenesis (see also Figs 5A, 6A). [Scale bars = 10 μm but D has its own scale bar].

opisthe (Fig. 6C). The developing anlage may not be perfectly synchronized as stomatogenesis is completed (Fig. 6D). The anterior end of the paroral appears to bend towards the left "carrying" the oral field with it as the oral cavity begins to invaginate (Figs 5, 6). By the time the cells are separating, the oral regions of the proter and opisthe have achieved their morphostatic form (Figs 5, 6).

Type host: *Fusiforma themisticola* n. gen., n. sp. was found throughout the haemocoel of the host hyperiid amphipod *Themisto libellula*, infecting 4.4% of the hosts examined (Prokopowicz et al. 2010). Intense infections were identified by observing the tips of appendages where densely packed ciliates could be observed through the thinner cuticle. Host amphipods were captured both in nets and in sediment traps: for a given host size, prevalence in nets was lower than in traps (i.e., 6% vs 16.3%), suggesting that these ciliates may kill their hosts (Prokopowicz et al. 2010).

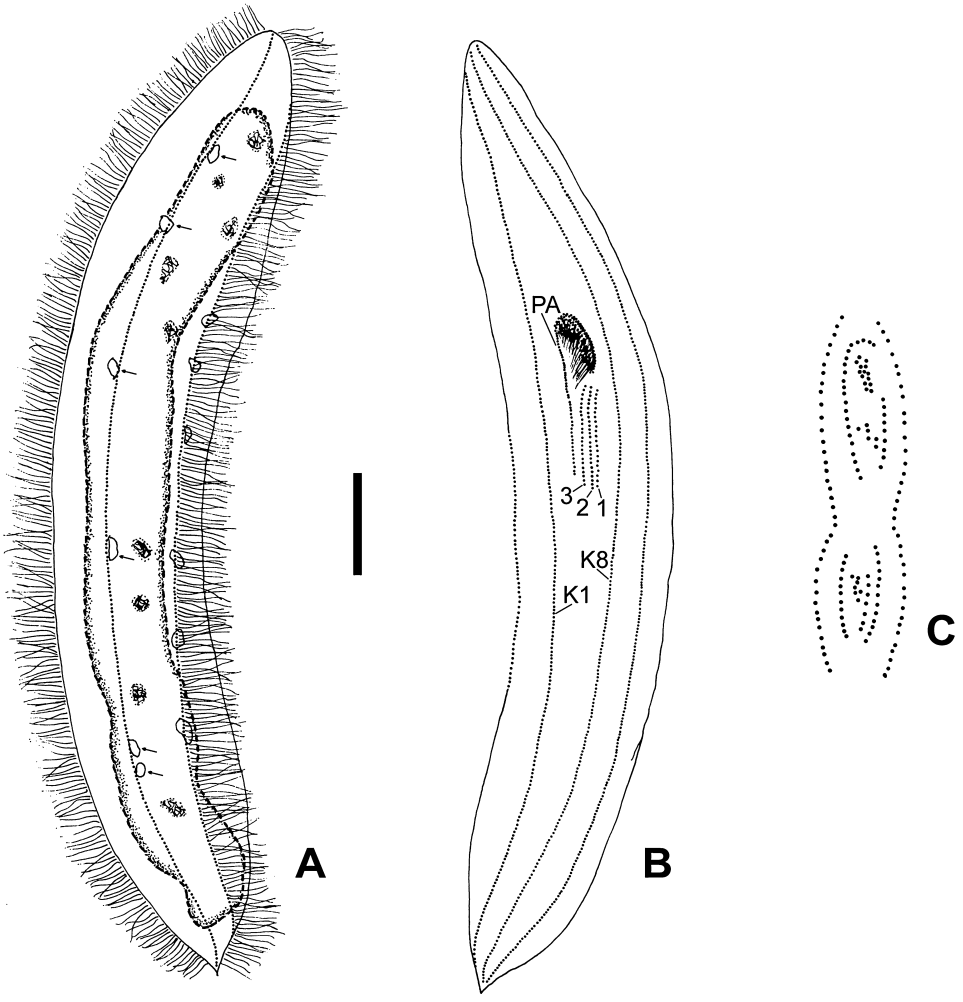

Figure 4. Schematic drawings of the type specimen of a protargol-stained *Fusiforma themisticola* n. gen., n. sp. **A**. Dorsal view of non-dividing cell illustrating dense ciliation of kineties and the large elongate macronucleus. Vesicle-like structures are distributed along each kinety (arrows). **B**. Ventral view of non-dividing cell illustrating the oral region with the anterior ciliated oral cavity bounded on the right and anteriorly by a paroral (PA) and posteriorly by three oral kineties (1, 2, 3). K1, K8 – somatic kineties 1 and 8. Scale bar = 10 μm for A and B. **C**. Detail of the oral regions of one of the smallest dividing cells observed. Note how few kinetosomes are involved in constructing the oral structures, suggesting that once division begins, it is a palintomic process without intervening kinetosomal replication. Not to scale.

Genetic Distance and Sequence Analyses

The partial SSU rRNA gene sequence of *Fusiforma themisticola* n. gen., n. sp. obtained from this study is 1,749 nucleotides in length and has a GC content of 41.1%. Genetic distance analyses were calculated from 1,541 unambiguously aligned nucleotide positions using several methods and nucleotide substitution models [i.e., number of base differences per sequence (no. of differences), number of base differences per site (*p*-distance), Jukes-Cantor (JC), Kimura two-parameter (K2P), Tajima-Nei (TN84), Tamura 3-parameter (T92), Tamura-Nei (TN93), LogDet (Tamura-Kumar), and Maximum Composite Likelihood (MCL)] implemented in the MEGA program. Mean numbers of base differences per sequence from averaging over all sequence pairs were 33.05 positions between *F. themisticola* and twenty pseudocolliniid isolates and 76.67 positions between *F. themisticola* and six foettingeriid isolates (Table 2). Averaged sequence divergences based on different substitution models ranged from 2.15-2.23% for the

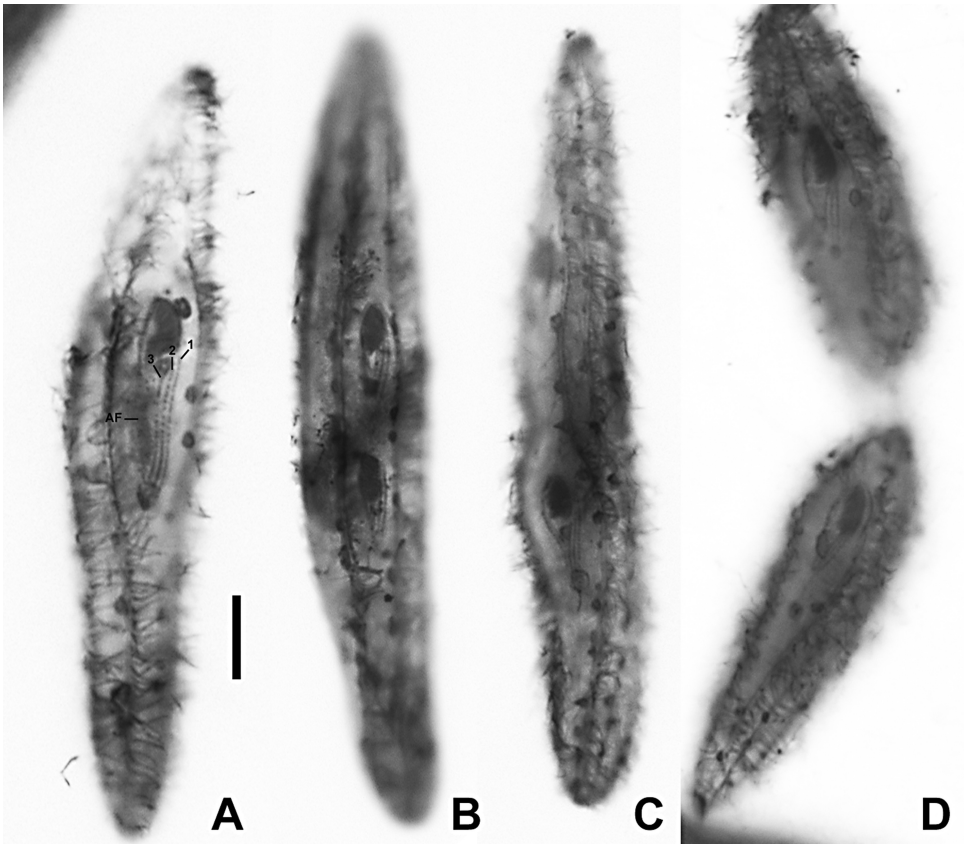

Figure 5. Protargol stains of dividing cells of *Fusiforma themisticola* n. gen., n. sp. **A**. Early divider in which the paroral has developed into an anarchic field (AF). The three oral kineties (1, 2, 3) appear to be elongating as the individual kinetosomes are now visible. **B**. Proter and opisthe oral fields have separated and the ciliature of the oral cavity is beginning to invaginate. **C**. Late stage of development of the opisthe oral region in which all the mature components are visible. **D**. Final separation of proter and opisthe. [Scale bar = 10 μm].

former and 5.01-5.49% for the latter pairs (Table 2). This suggests the closer genetic relationship of *F. themisticola* to the pseudocolliniids than to the foettingeriids. In addition, based on sequence analysis along 1,541 bp length of *F. themisticola*, twenty-six positions were shared between this novel ciliate and other pseudocolliniids but not foettingeriids, justifying establishment of the novel family

Table 2. Estimates of evolutionary divergences inferred from 1,541 nucleotide positions of the small subunit (SSU) rDNA among *Fusiforma themisticola* n. gen., n. sp., 20 pseudocolliniid isolates, and six foettingeriid isolates. The SSU rDNA sequence divergences were calculated with pairwise deletion in effect and shown in percentages except number of differences. The calculation is based on several methods and nucleotide substitution models [number of base differences per sequence (no. of differences), number of base differences per site (*p*-distance), Jukes-Cantor (JC), Kimura two-parameter (K2P), Tajima-Nei (TN84), Tamura 3-parameter (T92), Tamura-Nei (TN93), LogDet distance, and Maximum Composite Likelihood (MCL) models].

Taxa examined	*Fusiforma themisticola*								
	No. of differences	*p*-distance	JC	K2P	TN84	T92	TN93	LogDet	MCL
Pseudocolliniidae[a]	33.05	2.15	2.18	2.19	2.19	2.19	2.19	2.18	2.23
Foettingeriidae[b]	76.67	5.01	5.18	5.19	5.20	5.19	5.20	5.14	5.49

[a]included 20 SSU rDNA sequences of pseudocolliniid isolates.
[b]included six SSU rDNA sequences of foettingeriid isolates.

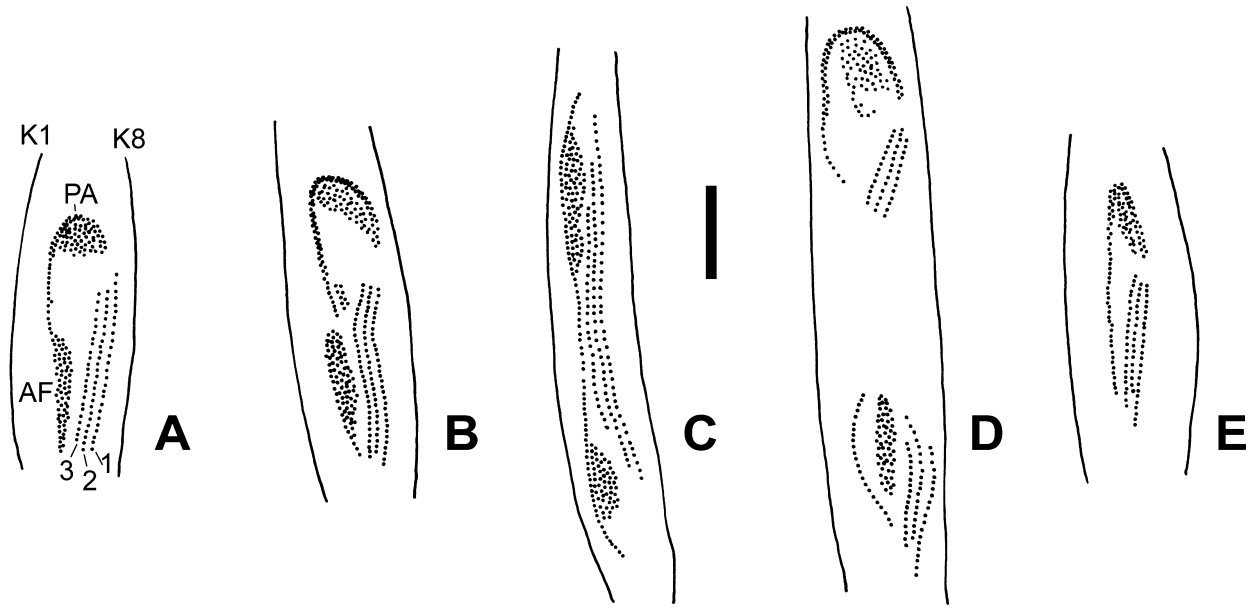

Figure 6. Schematic drawings of protargol-stained dividing *Fusiforma themisticola* n. gen., n. sp. **A**. Early division stage in which the posterior end of the paroral (PA) proliferates kinetosomes as an anarchic field (AF) for the oral cavity ciliature of the opisthe. The kinetosomes of the three oral kineties (1, 2, 3) appear to be more widely spaced. **B**. Separation and migration of the opisthe anarchic field occurs as the density of kinetosomes in the three oral kineties increases. **C**. The proter oral cavity has now dedifferentiated, the paroral has reached its elongated state as have the three oral kineties. **D**. The paroral of the proter has apparently wrapped around the anterior end of the oral field as the oral region reaches its mature extent. **E**. The oral region of a cell that is just about to separate from its partner. [Scale bar = 10 μm].

Pseudocolliniidae to include *Fusiforma* and *Pseudocollinia* (see Discussion). Furthermore, 12 sites were unique to *F. themisticola* and not found in any isolate of *Pseudocollinia*, substantiating establishment of the new genus *Fusiforma*.

Molecular Phylogenetic Position

Phylogenetic analyses inferred from SSU rDNA sequences representing eleven classes of the Ciliophora and two dinoflagellate outgroups showed that *Fusiforma themisticola* belongs to the class Oligohymenophorea with Bayesian posterior probability of 1.00 and PhyML bootstrap value of 55.3% (Fig. 7). Further analyses including almost all currently available oligohymenophorean genera indicated the robust phylogenetic affinity of this novel parasitic ciliate to members of the subclass Apostomatia with full posterior probability and PhyML bootstrap supports and showed its sister-taxon relationship to *Pseudocollinia brintoni* with relatively weak support values – Bayesian posterior probability of 0.79 and PhyML bootstrap value of 65.4% (Fig. 8). Comprehensive analyses covering all subclasses (except Peritrichia) within the class Oligohymenophorea and including various members of the subclass Apostomatia strongly confirmed the close phylogenetic relationship of *F. themisticola* to isolates of *Pseudocollinia* with high support values: Bayesian posterior probability of 0.99 and PhyML bootstrap value of 94.6% (Fig. 9). In addition, this new ciliate showed a very close relationship to members of Pseudocolliniidae and Foettingeriidae with full Bayesian and bootstrap support in all analyses. Additional analyses, including many uncultured apostomatid ciliate sequences obtained from infected copepod hosts and recently discovered by Guo et al. (2012), consistently demonstrated a close phylogenetic relationship between *F. themisticola* and *Pseudocollinia brintoni* with very strong support values – Bayesian posterior probability of 1.00 and PhyML bootstrap value of 96.1% (Fig. 10). *Fusiforma themisticola* was also closely related to an uncultured apostome recovered from the copepod *Calanus sinicus* with Bayesian posterior probability of 0.76 and PhyML bootstrap value of 50.8% (Fig. 10).

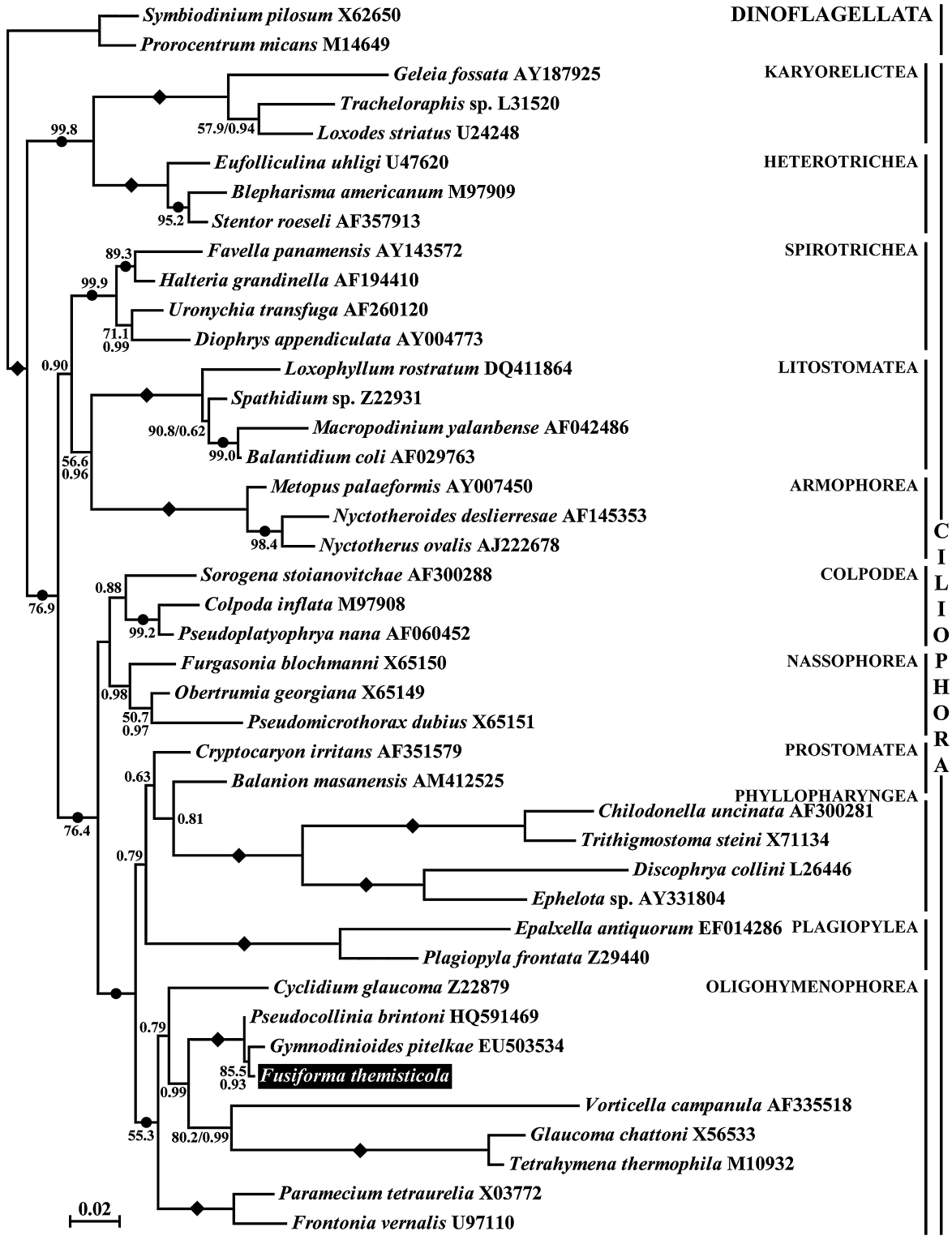

Figure 7. A maximum likelihood phylogenetic tree inferred from 1,226 unambiguously aligned sites of 42 small subunit (SSU) rDNA sequences, including 40 ciliate ingroup taxa covering representatives from all eleven classes of the phylum Ciliophora and two dinoflagellate outgroup taxa. The tree (ln *L* = -10180.376382) is constructed using PhyML with the GTR model of nucleotide substitution, estimated proportion of invariable

Discussion

Phylogenetic Position of Apostomatia

The apostomes have not always been considered related to the hymenostomes because their oral apparatus was apparently so divergent: Corliss (1979) among others placed them in the class Kinetofragminophora, a group of non-hymenostome ciliates. Small and Lynn (1981, 1985) transferred the apostomes to the class Oligohymenophorea, arguing that the somatic kinetids were similar to other oligohymenophoreans, and elevated the apostomes to subclass rank because of their derived features. Their life cycles show features typical of parasite-like hymenostomes and scuticociliates, and Bradbury (1989) demonstrated that the ultrastructural features of a paroral dikinetid are present during this life cycle. This, together with phylogenetic analyses of SSU rRNA genes, confirmed their placement with other oligohymenophoreans (Clamp et al. 2008; Gómez-Gutiérrez et al. 2012; this study). While the gene trees place the apostomes as sister to the scuticociliates, the genetic support for this relationship is not strong.

The morphology and stomatogenesis of *F. themisticola* provide further support for the relationship with the hymenostomes and the scuticociliates. This species is the first apostome to have a clearly differentiated paroral that borders the right and anterior sides of the oral cavity. Furthermore, during stomatogenesis, the posterior end of the paroral appears to function as a scutica, proliferating an anarchic field of kinetosomes that eventually become the kinetosomes of the left and anterior walls of the oral cavity (Lynn 2008; this study). The proter's left oral kineties of *F. themisticola* provide a direct continuity with those of the opisthe, merely elongating as the two oral fields separate and then breaking as the fission furrow begins to form. *Fusiforma themisticola* typically has three left oral kineties, which leads us to speculate that these may be the homologues of the *x*, *y*, and *z* kineties of foettingeriid apostomes (Bradbury et al. 1997; Chatton and Lwoff 1935).

Guo et al. (2012) analyzed the genetic diversity of apostome ciliates obtained from many copepod hosts based on SSU rRNA genes. These authors revealed significant hidden diversity among the apostomes, discovering several novel clades. However, only one clade – Group III as reported in Guo et al. (2012) – was grouped with two known apostome genera, *Gymnodinioides* and *Vampyrophrya* but without support. While there is no morphological characterization for a majority of these novel clades, our newly described *F. themisticola* did show a weak phylogenetic relationship with an undescribed apostome from the copepod *Calanus sinicus*.

A New Family of Apostomes – Pseudocolliniidae

Jankowski (2007) has most recently summarized his views on the taxonomy of the apostomes that are parasites of the haemolymph of crustaceans: he placed them in the monotypic order Colliniida Jankowski, 1980 with its single family Colliniidae Cépède, 1910. Jankowski (1980, 2007) analyzed the diversity in this family. He argued that the genus *Collinia* Cépède, 1910 should be divided into three genera. (1) The type species *Collinia circulans* (Fig. 11A) has trophonts that have 10 somewhat spiraled, somatic kineties that decrease in number with palintomy at the end of which oral fragments reminiscent of those of foettingeriids appear (i.e., *x*, *y*, and *z* kineties, possible rosette). (2) The trophonts of *Paracollinia* Jankowski, 1980 with its type species *Paracollinia branchiarum* (Stein, 1852) Jankowski, 1980 have numerous somatic kineties, sometimes up to 60, without a wide non-ciliated stripe, as in *Metacollinia* (see below). These kineties decrease in number to nine during palintomy at the end of which oral fragments reminiscent of those of foettingeriids appear (i.e., *x*, *y*, and *z* kineties, possible rosette) (Fig. 11B). (3) The trophonts of *Metacollinia* Jankowski, 1980 with its type species *Metacollinia luciensis* (Poisson, 1921) Jankowski, 1980 have numerous slightly spiraled, somatic kineties, sometimes up to 70, but have a dorsal non-ciliated stripe to differentiate them from *Paracollinia* spp. At the end of palintomy, during which kinety number decreases to nine, oral fragments reminiscent of those of foettingeriids appear (i.e., *x*, *y*, and *z* kineties, rosette)

sites and gamma shape parameter, and eight substitution rate categories implemented. Numbers on the branches indicate PhyML bootstrap percentages and Bayesian posterior probabilities higher than 50% or 0.50, respectively. Black circles represent Bayesian posterior probabilities of 1.00. Black diamonds represent PhyML bootstrap values of 100% and Bayesian posterior probabilities of 1.00. The scale bar corresponds to 0.02 substitutions per site. The sequence of *Fusiforma themisticola* n. sp. derived from this study is highlighted in the dark box.

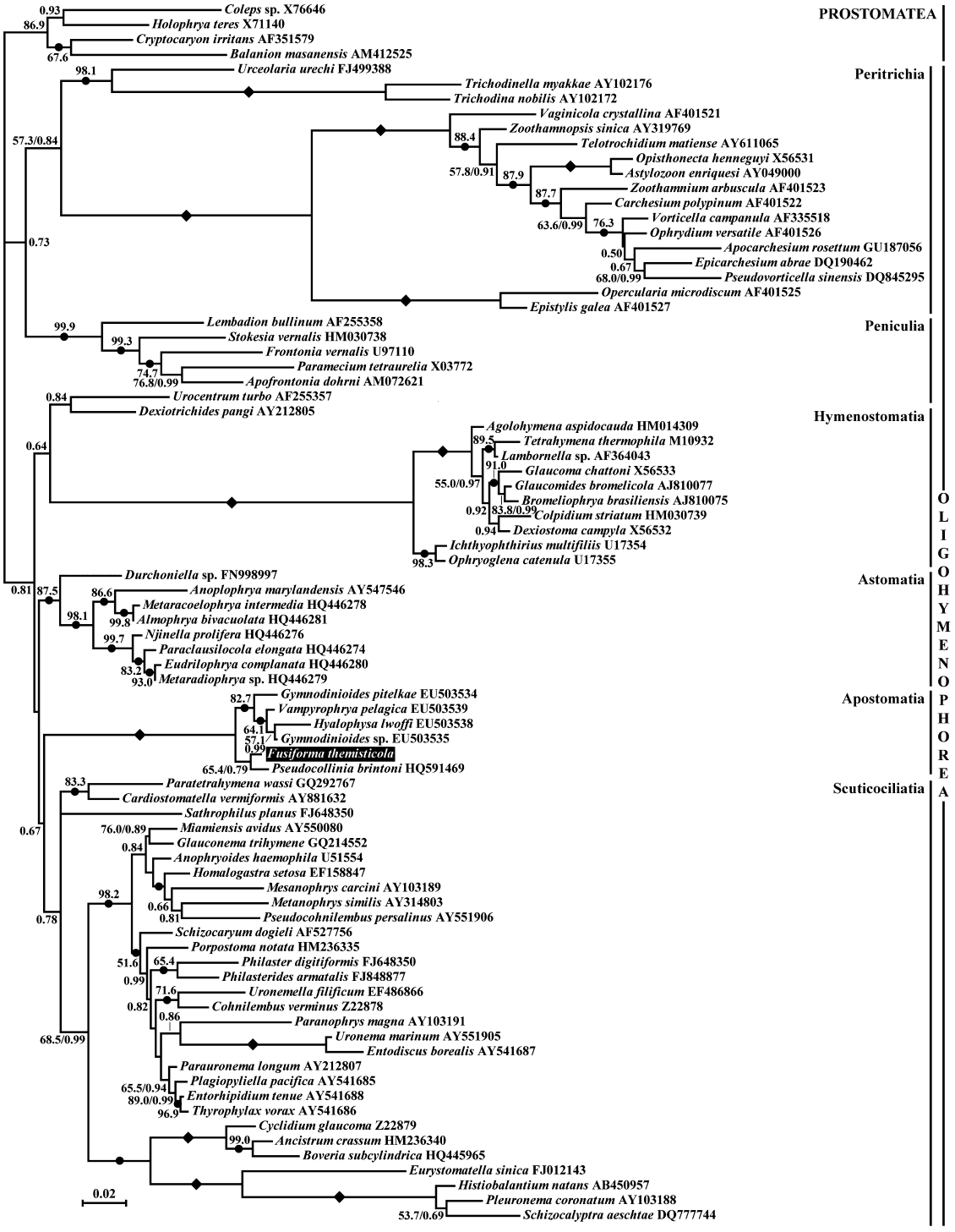

Figure 8. A maximum likelihood phylogenetic tree inferred from 1,580 unambiguously aligned sites of 82 small subunit (SSU) rDNA sequences, including all currently available representative genera of oligohymenophorean ciliate ingroup taxa and four prostomatean outgroup taxa. The tree (ln *L* = -18602.524867) is constructed using PhyML with the GTR model of nucleotide substitution, estimated proportion of invariable sites and gamma shape parameter, and eight substitution rate categories implemented. Numbers on the branches indicate PhyML bootstrap percentages and Bayesian posterior probabilities higher than 50% or 0.50, respectively.

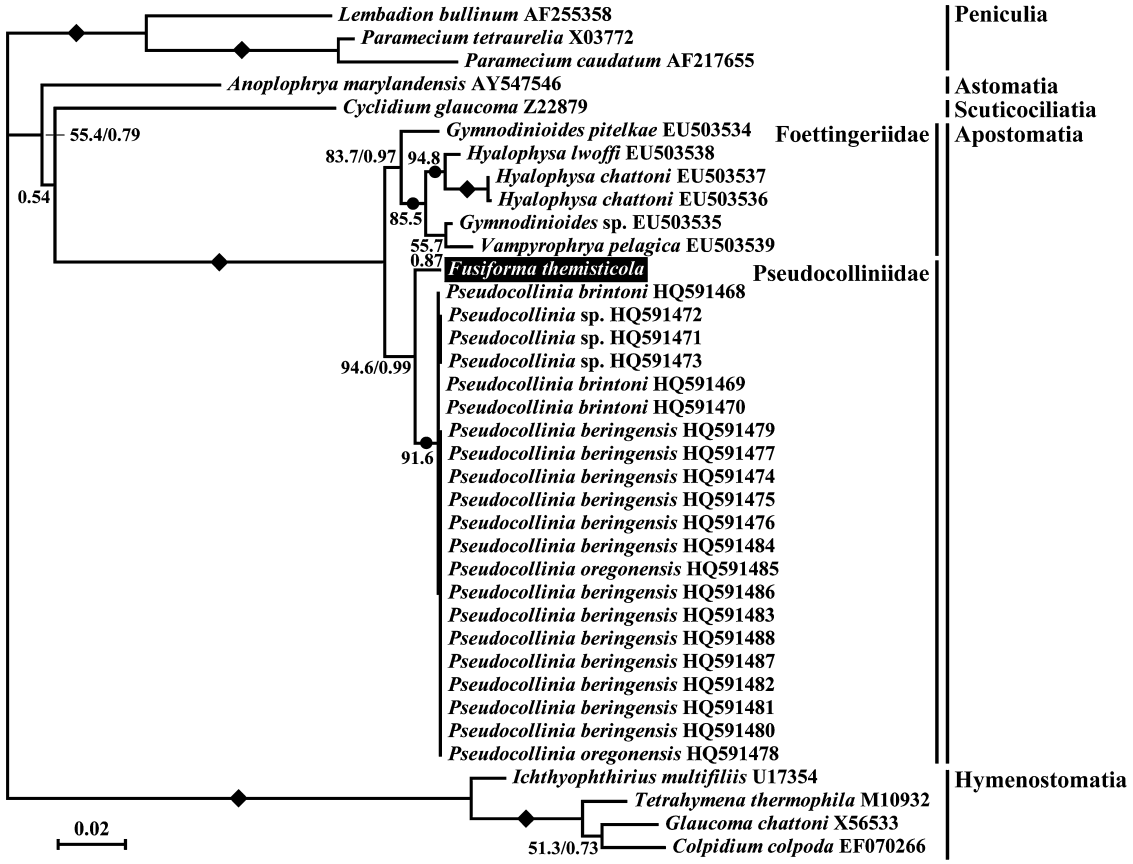

Figure 9. A maximum likelihood phylogenetic tree inferred from 1,658 unambiguously aligned sites of 37 small subunit (SSU) rDNA sequences, including several apostome ingroup taxa and three peniculian outgroup taxa. The tree (ln *L* = -6839.602825) is constructed using PhyML with the GTR model of nucleotide substitution, fixed proportion of invariable sites and estimated gamma shape parameter, and eight substitution rate categories implemented. Numbers on the branches indicate PhyML bootstrap percentages and Bayesian posterior probabilities higher than 50% or 0.50, respectively. Black circles represent Bayesian posterior probabilities of 1.00. Black diamonds represent PhyML bootstrap values of 100% and Bayesian posterior probabilities of 1.00. The scale bar corresponds to 0.02 substitutions per site. The sequence of *Fusiforma themisticola* n. sp. derived from this study is highlighted in the dark box.

(Fig. 11C, D). Thus, all three genera assigned by Jankowski (1980, 2007) to the family Colliniidae display oral fragments reminiscent of those of foettingeriids (i.e., *x*, *y*, and *z* kineties, rosette, and *r* kinety). For this reason, we think it is premature to segregate them into their own order, just on the basis of being haemolymph parasites.

On the other hand, species of *Pseudocollinia* and *Fusiforma* never display oral fragments similar to those of foettingeriids. Species in these genera, however, do have two or more left oral kineties that could be considered homologues of the *x*, *y*, and *z* kineties of foettingeriids: there are typically three of these left oral kineties in *F. themisticola* (Fig. 4B) and also three in *Pseudocollinia beringensis* (Fig. 11E) and two in *Pseudocollinia brintoni* (Fig. 11F). The permanent paroral or right oral kinety might be homologous to the *a* kinety that can appear, often transiently, during the life cycle of foettingeriids (Bradbury et al. 1997; Chatton and Lwoff 1935). We have not observed polymorphic life cycles in species of *Pseudocollinia* and *Fusiforma*,

Black circles represent Bayesian posterior probabilities of 1.00. Black diamonds represent PhyML bootstrap values of 100% and Bayesian posterior probabilities of 1.00. The scale bar corresponds to 0.02 substitutions per site. The sequence of *Fusiforma themisticola* n. sp. derived from this study is highlighted in the dark box.

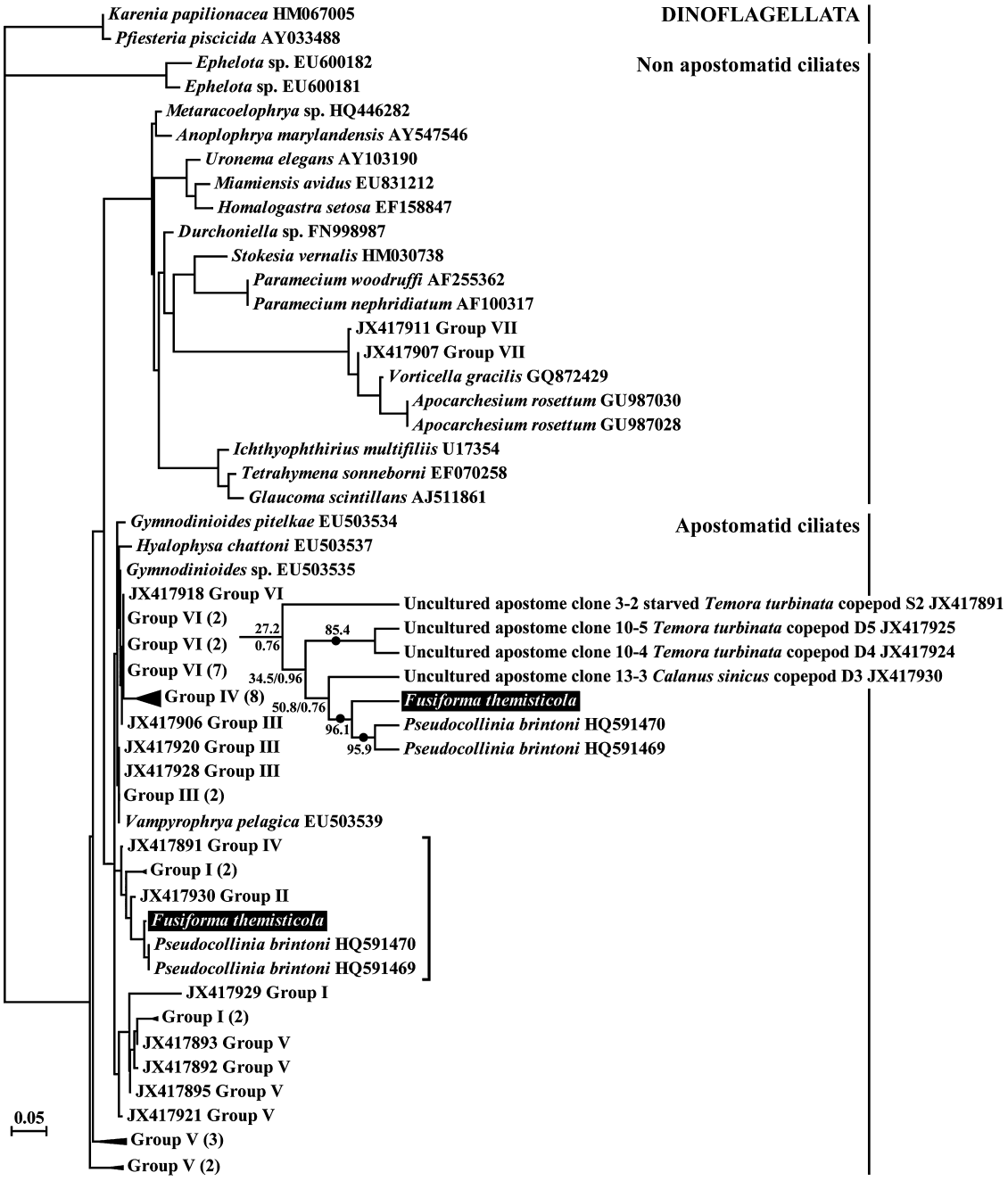

Figure 10. A maximum likelihood phylogenetic tree inferred from 594 unambiguously aligned sites of 69 small subunit (SSU) rDNA sequences, including many uncultured apostomatid ciliate sequences recently reported by Guo et al. (2012). The tree (ln *L* = -4628.574232) is constructed using PhyML with the TN93 model of nucleotide substitution, fixed proportion of invariable sites and gamma shape parameter, and eight substitution rate categories implemented. Support values are shown only in the clade containing *Fusiforma themisticola* n. sp. magnified from the taxa covered by the square bracket for clarity. Numbers on the branches indicate PhyML bootstrap percentages and Bayesian posterior probabilities, respectively. Group numbers were labeled for the taxa in the same way as those published by Guo et al. (2012) and, when more than one sequence was included, numbers of total sequences in those clades are given in parentheses after the group names. Black circles represent Bayesian posterior probabilities of 1.00. The scale bar corresponds to 0.05 substitutions per site. The sequence of *Fusiforma themisticola* n. sp. derived from this study is highlighted in the dark box.

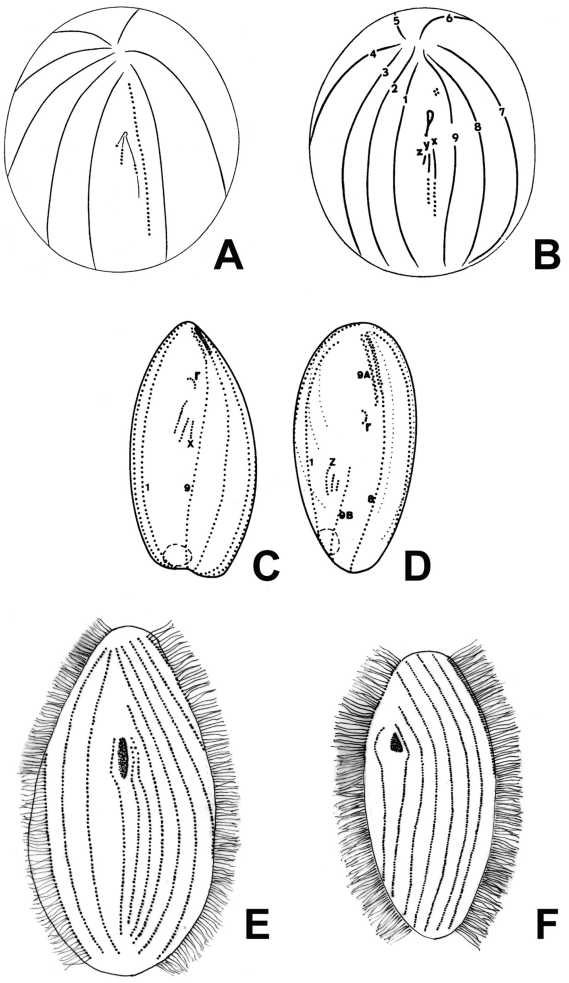

Figure 11. Schematic drawings of apostomes assigned to the families Colliniidae (A-D) and the new family Pseudocolliniidae n. fam. (E, F). **A**. Tomite of *Collinia circulans* (Balbiani, 1885) Jankowski, 2007 showing the rosette associated with three kinetofragments, presumably the *x*, *y*, and *z* kineties and an elongate kinety 9 (from fig. 14 of de Puytorac and Lom, 1962). **B**. Tomite of *Paracollinia branchiarum* (Stein, 1852) Jankowski, 1980, showing the *x*, *y*, and *z* kineties posterior to the loop-like rosette (from fig. 7 of de Puytorac and Lom, 1962). **C**, **D**. Protomite (C) and tomite (D) of *Metacollinia luciensis* (Poisson, 1921) Jankowski, 2007, showing the *x*, *y*, and *z* kineties, an *r* or "rosette" kinety, and differentiation of kinety 9 into A and B parts (from figures 14 and 15 of de Puytorac and Grain (1975) who described it as *Collinia orchestiae* from *Orchestia* sp. in France. Note that Jankowski (2007) considered this species synonymous with *Balantidium luciensis* Poisson, 1921, which was isolated from *Orchestia littorea* in France). **E**, **F**. Two species of the genus *Pseudocollinia* (compare to *Fusiforma themisticola*, Fig. 4B). **E**. *Pseudocollinia beringensis*, which has a single right oral kinety, which may be a homologue to the paroral, three left oral kineties, and a cone-shaped and ciliated oral cavity between the anterior ends of these oral kineties (from fig. 6 of Gómez-Gutiérrez et al. 2012). **F**. *Pseudocollinia brintoni*, which has a single right oral kinety, which may be a homologue to the paroral, two left oral kineties, and a cone-shaped and ciliated oral cavity between the anterior ends of these oral kineties (from fig. 6 of Gómez-Gutiérrez et al. 2012).

as has been observed in most other apostomes. We cannot definitively say that these are absent as we have not been able demonstrate a complete life cycle, possibly due to inadequate sampling (but see Gómez-Gutiérrez et al. 2012). Nevertheless, given the morphological differences between these two genera and other apostomes and the strong phylogenetic relationships between *Pseudocollinia* and *Fusiforma* in our molecular phylogenetic analyses, we propose the new family Pseudocolliniidae n. fam. with the type genus *Pseudocollinia* Gómez-Gutiérrez et al., 2012 to include also *Fusiforma* spp.

Subclass Apostomatia
Order Apostomatida
Family Pseudocolliniidae n. fam.

Diagnosis. Haemolymph-infesting parasites of crustaceans, such as amphipods and euphausiids, with a cup- or cone-shaped oral cavity whose left and anterior walls are covered by a dense field of ciliated kinetosomes; posterior to this oral cavity are one right oral kinety, which may become a paroral associated with the right and anterior borders of the oral cavity, and one to several left oral kineties; life cycles, while not completely determined, appear to involve only one host; varying degrees of polymorphism are exhibited by included genera.

Type genus. *Pseudocollinia* Gómez-Gutiérrez et al., 2012

Other included genera. *Fusiforma* n. gen.

A New Genus of Apostomes – *Fusiforma* n. gen.

We have described above the characteristics of a new genus and species of apostome – *Fusiforma themisticola* n. gen., n. sp. We have molecular genetic evidence based on the SSU rRNA gene that this ciliate is closely related to the parasitoid *Pseudocollinia* spp. that infect various species of krill in the Pacific Ocean. Furthermore, *Pseudocollinia* spp. and *F. themisticola* both have a

cone- or cup-shaped oral cavity whose left and anterior walls are covered by a dense field of ciliated kinetosomes and both taxa have oral kineties with those on the left outnumbering those on the right (Gómez-Gutiérrez et al. 2012). *Pseudocollinia* spp. differ from *F. themisticola* in several respects: *Pseudocollinia* spp. have (1) polymorphic life cycles with trophonts whose somatic kinety number increases with cell growth; (2) a right-hand oral kinety that while in the position of a paroral is never closely associated with the right and anterior borders of the oral cavity; and (3) have only been reported to infect krill species (Gómez-Gutiérrez et al. 2012 and references therein). While we do not yet have cytological evidence, our belief is that the trophonts of *Pseudocollinia* spp. undergo palintomic divisions without stomatogenesis and that the oral apparatus of protomites-tomites is differentiated at the last division whereas each palintomic division of *F. themisticola* is accompanied by stomatogenesis. Given these differences, we think that *F. themisticola* is justified as a new genus.

Fusiforma n. gen.

Diagnosis. Pseudocolliniid ciliates with paroral associated with a cone- or cup-shaped oral cavity and typically 3 (2-5) left oral kineties; somatic kinety number is typically 8 (6-9) densely ciliated kineties; haemolymph-infecting parasites, possibly parasitoids, of marine crustaceans.

Etymology. The etymology for the generic name, L. masc. *fusus* spindle; L. fem. *forma* shape. Feminine gender. The genus name reflects the spindle shape of the type species.

Type species. *Fusiforma themisticola* n. sp.

Type locality. Southeastern Beaufort Sea in the Canadian sector of the Arctic Ocean (132°–124° W; 70°–72° N) at the depth of 0–250 m.

Fusiforma themisticola n. sp.

Diagnosis. With features of the genus.

Etymology. The etymology for the specific epithet, *themisti-* referring to the host genus; L. *cola*, dweller, inhabitant. The specific epithet refers to the habitat of this species as the amphipod *Themisto*.

Type locality. Southeastern Beaufort Sea in the Canadian sector of the Arctic Ocean (132°–124° W; 70°–72° N) at the depth of 0–250 m, Canada. The host specimens, *Themisto libellula*, were collected at different times from September 2002 to August 2004.

Type host. *Themisto libellula* Lichtenstein, 1822 (Arthropoda, Crustacea, Amphipoda, Hyperiidea, Hyperiidae).

Habitat in host. Haemocoel and tissues surrounding the intestines of the amphipod hosts.

Holotype. A type slide (Accession No. USNM 1221443) of this ciliate species has been deposited in the Type Slide Collection of the Smithsonian Museum of Natural History, with the holotype circled in blank ink on this slide.

Hapantotype. Cells on gold sputter-coated SEM stubs have been deposited in the Beaty Biodiversity Research Centre (Marine Invertebrate Collection) at the University of British Columbia, Vancouver, Canada.

DNA sequence. Small subunit rRNA gene sequence [GenBank accession number KF516511].

Taxonomic Summary

Phylum Ciliophora Doflein, 1901

Subphylum Intramacronucleata Lynn, 1996

Class Oligohymenophorea de Puytorac, Batisse, Bohatier, Corliss, Deroux, Didier, Dragesco, Fryd-Vesavel, Grain, Groliére, Iftode, Laval, Roque, Savoie, and Tuffrau, 1974

Subclass Apostomatia Chatton and Lwoff, 1928

Order Apostomatida Chatton and Lwoff, 1928

Family Pseudocolliniidae n. fam. Chantangsi, Lynn, Rueckert, Prokopowicz, and Panha, 2013

Genus *Fusiforma* n. gen. Chantangsi, Lynn, Rueckert, Prokopowicz, Panha, and Leander, 2013

Species *Fusiforma themisticola* n. sp. Chantangsi, Lynn, Rueckert, Prokopowicz, Panha, and Leander, 2013

Methods

Sample collection: Several individuals of a novel parasitic ciliate *Fusiforma themisticola* were obtained from the haemocoel and tissues surrounding the intestines of the hyperiid amphipod *Themisto libellula* by opening the abdominal side of the crustaceans under a Leica MZ6 dissecting microscope. These amphipod hosts were collected at different periods from September 2002 to August 2004 from the Canadian Beaufort Sea (Arctic Ocean) using plankton nets and sediment trap sampling methods (see Prokopowicz et al., 2010 for further detailed information about sampling sites and specimen collection). Briefly, three sampling gears with different mesh sizes were deployed at various water depths — (1) a Kiel Hydrobios© multi-layer sampler equipped with nine 200-μm nets deployed from the bottom or a maximum depth of 200 m to the surface; (2) an E-Z-Net® multi-layer sampler armed with nine 333-μm

nets used from a depth of 250 m to the surface; and (3) a Double Square Net (DSN) equipped with two 750-μm nets down to a depth of 47 ± 8 m. The sediment samples for *T. libellula* were collected utilizing traps deployed in 100- or 200-m depths. Collected host specimens were immediately preserved in 5% (v/v) buffered formalin. The preserved specimens were dissected under a stereo microscope to disclose the gut and haemocoel contents of *T. libellula*. The ciliates were then isolated by micromanipulation using sterile glass Pasteur pipettes and stored in a clean vial containing 95% (v/v) ethanol for subsequent studies.

Cytological staining and light microscopy: The ciliates were removed from the formaldehyde-fixed infected hosts and underwent protargol staining using the Quantitative Protargol Stain as described by Montagnes and Lynn (1993) to reveal cellular and subcellular features, including nuclei, extrusomes, and microtubular constituents of the ciliate. Unstained formalin-fixed specimens were isolated and placed on a slide for light microscopy using differential interference contrast (DIC) microscopy with a Zeiss Axioplan 2 imaging microscope connected to a Leica DC500 color digital camera. Protargol-impregnated specimens were observed under a Leitz Aristoplan light microscope and photographed using a Leica DFC420 digital imaging camera to document morphological cellular features of the organisms. Cells oriented either dorsally or ventrally were measured using an ocular micrometer. Drawings of the stained ciliates were made by using a light microscope equipped with a drawing tube at 1,000X magnification.

Scanning electron microscopy (SEM): Formalin-fixed specimens of the ciliates were isolated in seawater by opening the body cavity of *T. libellula* under a Leica MZ6 dissecting microscope. The released material was examined under a Zeiss Axiovert 200 inverted microscope and ciliates were removed by micromanipulation and washed three times in seawater. Around 30 formalin-fixed ciliates were prepared for scanning electron microscopy (SEM). Isolated specimens were deposited directly into the threaded hole of a Swinnex filter holder, containing a 5-μm polycarbonate membrane filter (Millipore Corp., Billerica, MA), which was submerged in 10 ml of seawater within a small canister (2 cm diameter and 3.5 cm tall). A piece of Whatman No. 1 filter paper was mounted on the inside base of a beaker (4 cm dia. and 5 cm tall) that was slightly larger than the canister. The filter paper was saturated with 4% (w/v) OsO_4 and the beaker was turned over the canister. The ciliates were fixed by OsO_4 vapors for 30 min. Ten drops of 4% OsO_4 were added directly to the seawater and the ciliates were fixed for an additional 30 min. A 10-ml syringe filled with distilled water was screwed to the Swinnex filter holder and the entire apparatus was removed from the canister containing seawater and fixative. The ciliates were washed with distilled water then dehydrated with a graded series of ethyl alcohol and critical-point dried with CO_2. Filters were mounted on stubs, sputter coated with 5-nm gold, and viewed under a Hitachi S4700 scanning electron microscope. Some SEM images were presented on a black background using Adobe Photoshop 6.0 (Adobe Systems, San Jose, CA).

DNA extraction and PCR amplification: Ethanol-fixed cells of *Fusiforma themisticola* were isolated and their genomic DNA was extracted using the Total Nucleic Acid Purification kit by Epicentre (Madison, WI, USA). The extracted genomic DNA was employed as template for small subunit rRNA gene amplification using forward PF1 (5′-GCGCTACCTGGTTGATCCTGCC-3′) and reverse R4 primers (5′-GATCCTTCTGCAGGTTCACCTAC-3′) with an expected product of about 1,800 bp. A polymerase chain reaction (PCR) with the final reaction volume of 25 μl was performed in a thermal cycler using puReTaq Ready-To-Go PCR beads (GE Healthcare Bio-Sciences, Inc., Québec, Canada). The thermal cycler was programmed as follows: hold at 94 °C for 4 min; 5 cycles of denaturation at 94 °C for 30 sec, annealing at 45 °C for 1 min, and extension at 72 °C for 105 sec; 35 cycles of denaturation at 94 °C for 30 sec, annealing at 55 °C for 1 min, and extension at 72 °C for 105 sec; and hold at 72 °C for 10 min. A PCR band corresponding to the expected size was separated by agarose gel electrophoresis and then gel-purified with the UltraClean™ 15 DNA Purification Kit (MO BIO Laboratories, Inc., CA, USA). The cleaned DNA was cloned into pCR2.1 vector using the TOPO TA Cloning® kit (Invitrogen Corporation, CA, USA). Plasmids with the correct insert size were sequenced using BigDye 3.1 and the vector forward M13F (5′-GTAAAACGACGGCCAG-3′) and reverse M13R (5′-CAGGAAACAGCTATGAC-3′) primers and an internal 525F primer (5′-AAGTCTGGTGCCAGCAGCC-3′) with an Applied Biosystems 3730S 48-capillary sequencer. The SSU rRNA gene sequences were imported into Sequencher™ (version 4.5, Gene Codes Corporation, Ann Arbor, Michigan, USA), vector-trimmed at the ends, assembled into contigs, and visually checked for sequencing errors. The edited DNA sequence of the partial 1,749-bp SSU rRNA gene was deposited into GenBank (accession number KF516511).

Sequence alignment: Acquired sequences were initially identified by Basic Local Alignment and Search Tool (BLAST) analysis. The SSU rDNA sequence derived from *Fusiforma themisticola* was aligned with other ciliate ingroups and two dinoflagellate outgroups using MAFFT version 6 (Katoh and Toh 2008) and further inspected visually. The multiple sequence alignments were imported into the MEGA (Molecular Evolutionary Genetics Analysis) program version 5 (Tamura et al. 2011) and four alignments were created for phylogenetic analyses: (1) a 42-taxon alignment comprising 40 sequences of representatives from all 11 classes of ciliates plus two sequences of dinoflagellate outgroups (1,226 unambiguous sites); (2) an 82-taxon alignment comprising comprehensive sequences of almost all currently available oligohymenophorean genera (1,580 unambiguous sites) and covering representative members of all 6 subclasses of the Oligohymenophorea [i.e., Apostomatia, Astomatia, Hymenostomatia, Peniculia, Peritrichia, and Scuticociliatia] plus 4 sequences of prostomateans as the outgroup; (3) a 37-taxon ciliate alignment including *Fusiforma themisticola* and its closely related allies (1,658 unambiguous sites); and (4) a 69-taxon alignment including two sequences of dinoflagellate outgroups, *Fusiforma themisticola*, two sequences of *Pseudocollinia brintoni*, and 64 ciliate sequences in the same taxon composition as published in figure 3 by Guo et al. (2012) (594 unambiguous sites). All highly variable and ambiguously aligned sites were excluded from the alignments prior to phylogenetic analyses. All alignment files are available upon request.

Sequence analyses: A dataset comprising SSU rDNA sequences of apostomatid ciliates was constructed and aligned to determine genetic distance among members within the group and to reveal unique molecular signatures of the newly described *Fusiforma themisticola* n. gen., n. sp. This dataset included the following: *Fusiforma* (1 sequence: *F. themisticola*), *Gymnodinioides* (2: *G. pamlico* and *G. pitelkae*), *Hyalophysa* (3: 2 of *H. chattoni* and *H. lwoffi*), *Pseudocollinia* (20: 13 of *P. beringensis*, 2 of *P. brintoni*, 2 of *P. oregonensis*, and 3 of *Pseudocollinia* spp.), and *Vampyrophrya* (1: *V. pelagica*). A total of twenty-seven sequences and 1,541 unambiguously aligned sites were included in these analyses. Sequence divergences were calculated with the MEGA version 5 program using number of base differences per sequence (no. of differences), number of base differences per site (*p*-distance),

Jukes-Cantor (JC) (Jukes and Cantor 1969), Kimura two-parameter (K2P) (Kimura 1980), Tajima-Nei (TN84) (Tajima and Nei 1984), Tamura 3-parameter (T92) (Tamura 1992), Tamura-Nei (TN93) (Tamura and Nei 1993), LogDet (Tamura-Kumar) (Tamura and Kumar 2002), and Maximum Composite Likelihood (MCL) (Tamura et al. 2004) models with pairwise deletion in effect. All ambiguous or gap positions were removed for each sequence pair or deleted in pairwise manner when analyses were performed.

Phylogenetic analyses: Phylogenetic trees were deduced using maximum likelihood (ML) and Bayesian inference (BI) methods in programs MrBayes version 3.1.2 (Huelsenbeck and Ronquist 2001; Ronquist and Huelsenbeck 2003) and PhyML version 3.0 (Guindon et al. 2010). The jModeltest program was employed to statistically select the best-fit model of nucleotide substitution with Akaike information criteria (AIC) calculation for the four constructed datasets (Posada 2008). For Bayesian analyses, four Markov Chain Monte Carlo (MCMC) chains — 1 cold chain and 3 heated chains — were performed for two parallel runs, each for 5,000,000 generations, sampling every 50th generation (tree). The first 25% or 25,000 trees were discarded as burn-in. The remaining trees were used to compute the 50% majority-rule consensus tree and posterior probabilities from both runs. Branch lengths of the trees were saved. Maximum likelihood analyses were conducted on the built datasets. The General Time Reversible (GTR) model was used in the 42-, the 82-, and the 37-taxon datasets and the Tamura-Nei (TN93) model was used in the 69-taxon dataset, all with optimized equilibrium base frequencies, estimated proportion of invariable sites and gamma shape parameter, and eight substitution rate categories as chosen by the modeling, except for the 37-taxon and 69-taxon datasets for which proportion of invariable sites was fixed as recommended by the jModeltest analysis. The input tree was estimated using BIONJ with NNI (Nearest Neighbor Interchange) and SPR (Subtree Pruning and Regrafting) as tree topology improvement methods and with 9 initial random starting trees implemented, except for the 69-taxon dataset for which 10 initial random starting trees were implemented. Optimization of topology and branch lengths was also performed. Support for ML topologies was evaluated from 1,000 bootstrap replicates using the same parameters described above.

Acknowledgements

We are grateful to Denis Tikhonenkov for his translation of the Russian text of Jankowksi (2007) and Michaela C. Strüder-Kypke for preparing the protargol stains of the formaldehyde-fixed material. C. Chantangsi and S. Panha were supported by a grant to C. Chantangsi from the Thailand Research Fund (TRF: MRG5580155); C. Chantangsi was also supported by a grant to BSL from the Natural Science and Engineering Research Council (NSERC) of Canada Grant 283091-09. D. H. Lynn and M. C. Strüder-Kypke were supported by a NSERC of Canada Discovery Grant awarded to DHL. A. J. Prokopowicz was supported by the NSERC of Canada. S. Rueckert was supported by a grant to BSL from the Tula Foundation's Centre for Microbial Diversity and Evolution. BSL was also supported by the Canadian Institute for Advanced Research, Program in Integrated Microbial Biodiversity. Finally, we are thankful to two anonymous reviewers for their constructive and helpful comments on the earlier draft of the article.

References

Arthur JR, Lom J (1984) Trichodinid protozoa (Ciliophora: Peritrichida) from freshwater fishes of Rybinsk Reservoir, USSR. J Protozool **31**:82–91

Bradbury PC (1989) Evidence for hymenostome affinities in an apostome ciliate. J Protozool **36**:95–103

Bradbury PC, Song W, Zhang L (1997) Stomatogenesis during the formation of the tomite of *Hyalophysa chattoni* (Hymenostomatida: Ciliophora). Eur J Protistol **33**:409–419

Chatton E, Lwoff A (1935) Les ciliés apostomes. Morphologie, cytologie, éthologie, évolution, systématique. Première partie. Aperçu historique et général. Étude monographique des genres et des espèces. Arch Zool Exp Gén **77**:1–453

Clamp JC, Bradbury PC, Strüder-Kypke MC, Lynn DH (2008) Phylogenetic position of the apostome ciliates (phylum Ciliophora, subclass Apostomatia) tested using small subunit rRNA gene sequences. Denisia **23**:395–402

Corliss JO (1979) The Ciliated Protozoa: Characterization, Classification, and Guide to the Literature. 2nd ed. Pergamon Press, London and New York, 455 p

de Puytorac P, Grain J (1975) Étude de la tomitogenèse et de l'ultrastructure de *Collinia orchestiae*, cilié apostome sanguicole, endoparasite du crustacé *Orchestia gammarella* Pallas. Protistologica **11**:61–74

de Puytorac P, Lom J (1962) La tomitogenèse des *Collinia* ciliés apostomes sanguicoles endoparasites des crustacés. Ann Parasitol Humaine Comp **37**:195–209

Dickerson HW, Dawe DL (1995) *Ichthyophthirius multifiliis* and *Cryptocaryon irritans* (Phylum Ciliophora). In Woo PTK (ed) Fish Diseases and Disorders. Protozoan and Metazoan Infections. Vol 1. CAB International, Wallingford, Washington, pp 181–227

Fernandez-Leborans G, Tato-Porto ML (2000) A review of the species of protozoan epibionts on crustaceans. I. Peritrich ciliates. Crustaceana **73**:643–683

Gómez-Gutiérrez J, Peterson WT, De Robertis A, Brodeur RD (2003) Mass mortality of krill caused by parasitoid ciliates. Science **301**:339

Gómez-Gutiérrez J, Strüder-Kypke MC, Lynn DH, Shaw TC, Aguilar-Méndez MJ, López-Cortés A, Martínez-Gómez S, Robinson CJ (2012) *Pseudocollinia brintoni* gen. nov., sp. nov. (Apostomatida: Colliniidae), a parasitoid ciliate infecting the euphausiid *Nyctiphanes simplex*. Dis Aquat Org **99**:57–78

Guindon S, Dufayard JF, Lefort V, Anisimova M, Hordijk W, Gascuel O (2010) New algorithms and methods to estimate maximum-likelihood phylogenies: assessing the performance of PhyML 3.0. Syst Biol **59**:307–321

Guo Z, Liu S, Hu S, Li T, Huang Y, Liu G, Zhang H, Lin S (2012) Prevalent ciliate symbiosis on copepods:

high genetic diversity and wide distribution detected using small subunit ribosomal RNA gene. PLoS ONE **7**:e44847, http://dx.doi.org/10.1371/journal.pone.0044847

Hoffman GL (1988) Ciliates of Freshwater Fishes. In Kreier P (ed) Parasitic Protozoa. Vol 2. Academic Press, New York, pp 583–632

Huelsenbeck JP, Ronquist F (2001) MrBayes: Bayesian inference of phylogenetic trees. Bioinformatics **17**:754–755

Jankowski AW (1980) Conspectus of a new system of the phylum Ciliophora. Trudy Zool Inst Leningrad **94**:103–121 (in Russian)

Jankowski AW (2007) Phylum Ciliophora Doflein, 1901. In Alimov AF (ed) Protista, Part 2, Handbook on Zoology. Russian Academy of Sciences, Zoological Institute, St. Petersburg, pp 415–993 (in Russian with English summary)

Jukes TH, Cantor CR (1969) Evolution of Protein Molecules. In Munro HN (ed) Mammalian Protein Metabolism. Academic Press, New York, pp 21–132

Katoh K, Toh H (2008) Recent developments in the MAFFT multiple sequence alignment program. Brief Bioinform **9**:286–298

Kimura M (1980) A simple model for estimating evolutionary rates of base substitutions through comparative studies of nucleotide sequences. J Mol Evol **16**:111–120

Landers SC (2010) The fine structure of the hypertrophont of the parasitic apostome *Synophrya* (Ciliophora, Apostomatida). Eur J Protistol **46**:171–179

Lom J (1995) Trichodinidae and Other Ciliates (Phylum Ciliophora). In Woo PTK (ed) Fish Diseases and Disorders. Protozoan and Metazoan Infections Vol 1. CAB International, Wallingford, Washington, pp 229–262

Lynn DH (2008) The Ciliated Protozoa: Characterization, Classification, and Guide to the Literature. 3rd ed Springer, Dordrecht, 606 p

Montagnes DJS, Lynn DH (1993) A quantitative Protargol Stain (QPS) for Ciliates and Other Protists. In Kemp P, Sherr B, Sherr E, Cole J (eds) Aquatic Microbial Ecology. Lewis Publishers, London, UK, pp 229–240

Pérez JM (2009) Parasites, pests, and pets in a global world: New perspectives and challenges. J Exot Pet Med **18**:248–253

Posada D (2008) jModelTest: phylogenetic model averaging. Mol Biol Evol **25**:1253–1256

Prokopowicz AJ, Rueckert S, Leander BS, Michaud J, Fortier L (2010) Parasitic infection of the hyperiid amphipod *Themisto libellula* in the Canadian Beaufort Sea (Arctic Ocean), with a description of *Ganymedes themistos* sp. n. (Apicomplexa, Eugregarinorida). Polar Biol **33**:1339–1350

Ronquist F, Huelsenbeck JP (2003) MRBAYES 3: Bayesian phylogenetic inference under mixed models. Bioinformatics **19**:1572–1574

Small EB, Lynn DH (1981) A new macrosystem for the Phylum Ciliophora Doflein, 1901. BioSystems **14**:387–401

Small EB, Lynn DH (1985) Phylum Ciliophora Doflein, 1901. In Lee JJ, Hutner SH, Bovee EC (eds) An Illustrated Guide to the Protozoa. Society of Protozoologists, Lawrence, Kansas, pp 393–575

Tajima F, Nei M (1984) Estimation of evolutionary distance between nucleotide sequences. Mol Biol Evol **1**:269–285

Tamura K (1992) Estimation of the number of nucleotide substitutions when there are strong transition-transversion and G + C-content biases. Mol Biol Evol **9**:678–687

Tamura K, Kumar S (2002) Evolutionary distance estimation under heterogeneous substitution pattern among lineages. Mol Biol Evol **19**:1727–1736

Tamura K, Nei M (1993) Estimation of the number of nucleotide substitutions in the control region of mitochondrial DNA in humans and chimpanzees. Mol Biol Evol **10**:512–526

Tamura K, Nei M, Kumar S (2004) Prospects for inferring very large phylogenies by using the neighbor-joining method. Proc Natl Acad Sci USA **101**:11030–11035

Tamura K, Peterson D, Peterson N, Stecher G, Nei M, Kumar S (2011) MEGA5: Molecular evolutionary genetics analysis using maximum likelihood, evolutionary distance, and maximum parsimony methods. Mol Biol Evol **28**:2731–2739